# Examination of the species and beam energy dependence of particle spectra using Tsallis statistics



2010 J. Phys. G: Nucl. Part. Phys. 37 085104

(http://iopscience.iop.org/0954-3899/37/8/085104)

IOP Publishing — Journal of Physics G: Nuclear and Particle Physics

J. Phys. G: Nucl. Part. Phys. **37** (2010) 085104 (10pp) doi:10.1088/0954-3899/37/8/085104

# Examination of the species and beam energy dependence of particle spectra using Tsallis statistics

**Ming Shao[1], Li Yi[1], Zebo Tang[1], Hongfang Chen[1], Cheng Li[1] and Zhangbu Xu[1,2]**

[1] Department of Modern Physics, University of Science and Technology of China, 96 Jinzhai Road, Hefei, Anhui 230026, People's Republic of China
[2] Brookhaven National Laboratory, Upton, NY 11973, USA

E-mail: zbtang@mail.ustc.edu.cn

Received 7 December 2009
Published 16 June 2010
Online at stacks.iop.org/JPhysG/37/085104

**Abstract**

Tsallis statistics was used to investigate the non-Boltzmann distribution of particle spectra and their dependence on particle species and beam energy in the relativistic heavy-ion collisions at SPS and RHIC. Produced particles are assumed to acquire radial flow and be of non-extensive statistics at freeze-out. $J/\psi$, and the particles containing strangeness were examined separately to study their radial flow and freeze-out. We found that the strange hadrons approach equilibrium quickly from peripheral to central A+A collisions and they tend to decouple earlier from the system than the light hadrons but with the same final radial flow. These results provide an alternative picture of freeze-outs: a thermalized system is produced at the partonic phase; the hadronic scattering at a later stage is not enough to maintain the system in equilibrium and does not increase the radial flow of the copiously produced light hadrons. The $J/\psi$ in Pb+Pb collisions at SPS is consistent with early decoupling and obtains little radial flow. The $J/\psi$ spectra at RHIC are also inconsistent with the bulk flow profile.

(Some figures in this article are in colour only in the electronic version)

## 1. Introduction

Identified particle spectra in transverse momenta are one of the pillars in the major discoveries in high-energy nuclear physics [1–4]. It has been demonstrated that the spectral shape is sensitive to the dynamics of the nucleus–nucleus collisions [5, 6] and can be used to obtain the radial flow and temperature at freeze-out. In addition, it has been argued that hadrons containing strange or charm valence quarks should have smaller hadronic interaction cross-section, and should decouple from the system earlier than the hadrons with only light valence quarks [1, 5, 6]. In this scenario, those strange and charmed hadrons would carry direct information from the collisions at an earlier stage without dilution due to hadronic scattering at the later stage. Particle spectra at SPS and RHIC have been used to extract this behavior [5, 6]. The Boltzmann–Gibbs blast-wave (BGBW) model distribution has been applied to SPS and RHIC data, and was the basis for the observation of the early decoupling of multi-strange hadrons [5, 6]. On the other hand, the evolution with hydrodynamics shows that the multi-strange particle spectra can be well described by the same hydrodynamics at the same freeze-out as other hadrons [7].

Recently, non-extensive hydrodynamics has been proposed to explain some essential features in relativistic heavy-ion collisions [8–17]. A simplified model with blast-wave assumption and non-extensive Tsallis statistics for hadrons at freeze-out has been implemented and applied successfully to describe the RHIC data including all the multi-strange hadrons up to intermediate $p_T$ [10]. The same approach was extended to fit the hadron spectra at SPS [18]. Although it was concluded in [10] that a common non-extensive Tsallis blast-wave (TBW) model can describe hadrons with and without strange valence quarks, it was claimed in [18] that multi-strange hadrons and $J/\psi$ freeze out at much higher temperature and acquire smaller radial flow than light hadrons.

In this paper, we perform a systematic study of hadron spectra at SPS and RHIC top energies with TBW as in [10]. Detailed comparisons of spectral shape from the model and data are carried out to assess the degree of this discrepancy. In addition, we categorize the spectra into all hadrons, strange hadrons, non-strange hadrons and $J/\psi$ in an attempt to compare their spectral shapes to the TBW results.

## 2. TBW and its fit to RHIC and SPS data

The same TBW as in [10] is used in the current analyses:

$$\frac{\mathrm{d}N}{m_T\,\mathrm{d}m_T} \propto m_T \int_{-Y}^{+Y} \cosh(y)\,\mathrm{d}y \int_{-\pi}^{+\pi} \mathrm{d}\phi \int_0^R r\,\mathrm{d}r \times \left(1 + \frac{q-1}{T}(m_T\cosh(y)\cosh(\rho) - p_T\sinh(\rho)\cos(\phi))\right)^{-1/(q-1)}, \quad (1)$$

where the left-hand side is an invariant differential particle yield at mid-rapidity, $m_T$ and $p_T$ are the transverse mass and transverse momentum of the produced particle, $q$ is the parameter characterizing the degree of non-equilibrium and $\rho$ is the flow profile growing as the $n$th power ($n = 1$) along the transverse radial direction ($r$) from zero at the center of the collisions to $\beta_s$ at the hard-spherical edge ($R$).

The STAR Collaboration has published a series of particle spectra at mid-rapidity. The most complete set is for $p$+$p$ and Au+Au collisions at $\sqrt{s_{NN}} = 200$ GeV. The identified particle spectra include $\pi^\pm$, $K^\pm$, $K_S$, $K^*$, $p$, $\phi$, $\Lambda$, $\Xi$, $\Omega$, $\bar{p}$, $\bar{\Lambda}$, $\bar{\Xi}$ and $\bar{\Omega}$ [1, 19–27]. In addition, the PHENIX Collaboration has published the spectra of charged kaons [28] and $J/\psi$ [29–31], which are not included in the previous fits [10]. The charged kaon spectra from PHENIX Collaboration extend the STAR measurement to higher $p_T$. This is crucial for the current study when the spectra are categorized into several groups. In the group of hadrons with strange valence quarks, kaon is the only light meson whose spectrum is more sensitive to the non-equilibrium effect at low $p_T$ since the spectra of heavier particles are usually overwhelmed by radial flow in the low $p_T$ to intermediate $p_T$ in the central nucleus–nucleus collisions. $J/\psi$ spectra are measured by PHENIX Collaboration in $p$+$p$, Cu+Cu and Au+Au collisions at RHIC top energy for $p_T < 5$ GeV/$c$ [29–31] while STAR Collaboration has extended these measurements to high $p_T$ [32]. Only PHENIX data with $p_T < 5$ GeV/$c$ are used in this TBW

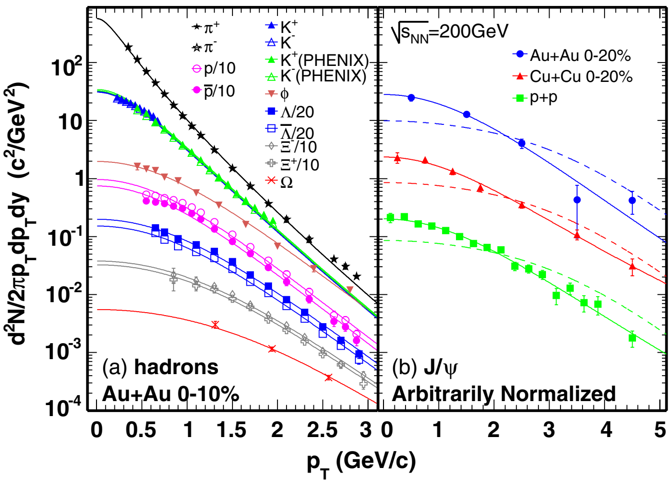


**Figure 1.** Identified particle spectra from Au+Au collisions at $\sqrt{s_{NN}}$ = 200 GeV. Left panel: spectra of light hadrons and strange hadrons. The solid curves are results from the TBW fit. Right panel: $J/\psi$ spectrum, the dashed line is the TBW prediction using parameters from the fit to other hadrons, and the solid curve is a TBW fit to $J/\psi$ alone.

analysis. We perform a TBW fit using (1). The procedure and program are described in detail in [10, 33].

Figure 1 shows the identified spectra measured by STAR and PHENIX Collaborations and their associated TBW curves from the fit. The yields are presented in terms of the invariant differential cross-section. There are a few features: the extension of kaon spectra to high $p_T$ does not change the quality of the fit and the kaon spectra can be well described by the TBW. However, using the same parameters from the fit, the TBW curve cannot reproduce the $J/\psi$ spectra as shown in the right panel of figure 1. The curve is too flat at low $p_T$, presumably due to the effect of large radial flow. We performed a TBW fit to the $J/\psi$ spectra alone. The result shows that $J/\psi$ has consistently lower radial flow than the bulk, although the parameter uncertainty is quite large due to the large statistical uncertainties of the data points.

Similarly, the same TBW fit was applied to SPS data [34–42]. Figure 2 shows the measured spectra together with the fit TBW curves for central Pb+Pb and In+In collisions at $\sqrt{s_{NN}}$ = 17.2 GeV. The TBW results are generally in good agreement with the data points. However, the $\chi^2$/nDoF is not as good as the fit at RHIC. Although the TBW curves represent the trends of the data points very well, the variations of the data points around the curves seem to be larger than those allowed by the error bars, indicating a possible underestimate of the uncertainties. In the right panel of figure 2, the $J/\psi$ data points from NA50 and NA60 were presented as a function of $p_T$ together with the TBW curves. The dashed line is the prediction using the parameters produced by the TBW fit to the other light hadrons, while the solid curve is a TBW fit to the $J/\psi$ spectrum alone. The same situation as observed at RHIC, the TBW prediction with parameters obtained from the fit to the light hadron spectra, overpredicts the radial flow present in the $J/\psi$ spectrum. A fit to the $J/\psi$ spectrum alone shows that the radial flow of $J/\psi$ at SPS is consistent with zero.

To further investigate the effect of the correlation between $T$ and $q$ as a potential cause for the large uncertainties from the $J/\psi$ fit, we examine the contour plot from the TBW fit to the $J/\psi$ spectra. The $J/\psi$ spectrum in $p$+$p$ collisions at $\sqrt{s}$ = 200 GeV has much smaller uncertainties with many more data points than those in A+A collisions at RHIC. We perform a

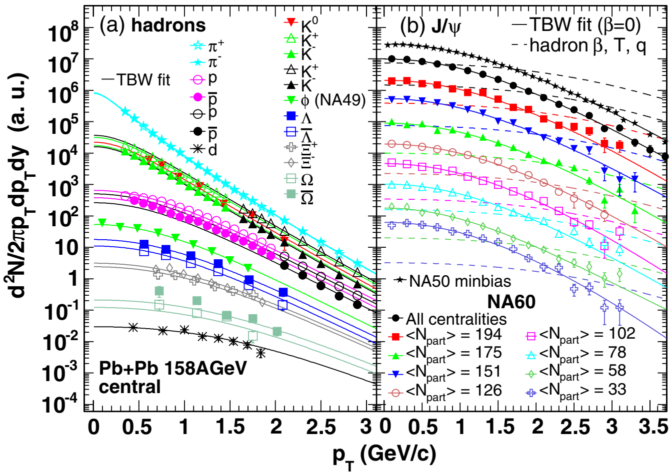


**Figure 2.** Identified particle spectra in central Pb+Pb collisions at the beam energy of 158 A GeV from the fixed-target experiments at SPS. Left panel: spectra of light hadrons and strange hadrons. The solid curves are results from the TBW fit. Right panel: $J/\psi$ spectra, the dashed line is the TBW prediction using parameters from the fit to other hadrons, and the solid curve is a TBW fit to $J/\psi$ alone.

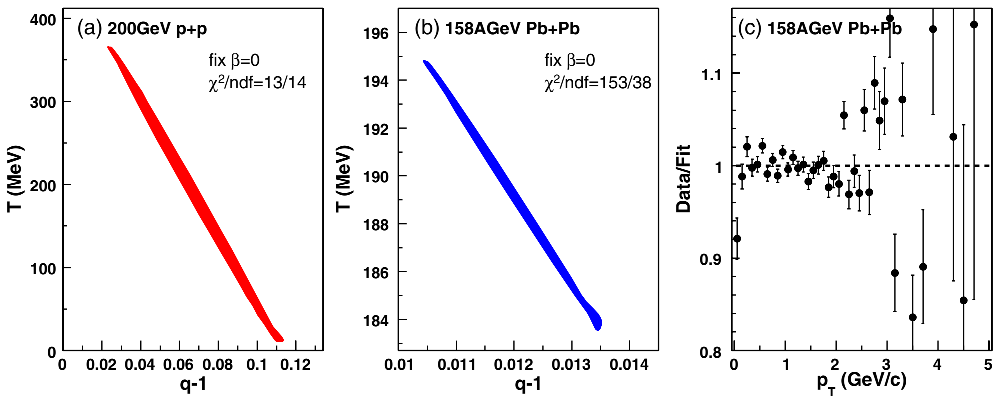


**Figure 3.** 1-$\sigma$ contour of the $T$ versus $(q-1)$ plane from the TBW fit to the $J/\psi$ spectrum in $p$+$p$ collisions at $\sqrt{s}$ = 200 GeV with $\chi^2$/nDoF = 13/14 at minimum (a), Pb+Pb collisions at $\sqrt{s_{NN}}$ = 17.2 GeV with $\chi^2$/nDoF = 153/38 (b) and ratio of data points to fit in Pb+Pb collisions (c). The radial flow is set to zero in this fit.

fit by setting radial flow to zero while only keeping $T$ and $q$ as free parameters. Figure 3 shows the 1-$\sigma$ contour of the $T$ versus $(q-1)$ plane with the best fit as presented in figures 1 and 2. It is obvious from the plot that there is a strong correlation between these two parameters. Once one parameter is constrained accurately by other means or other hadron spectra, the other parameter is also well constrained.

Intuitively, one expects that the strange hadrons with smaller hadronic interaction cross-sections would freeze out earlier than the bulk of hadrons [5]. This results in higher temperature and smaller radial flow for strange hadrons than for light hadrons without strange content. To study this effect, the particles are further grouped according to their species: all hadrons, strange hadrons and non-strange hadrons. Table 1 shows the fit results for these groups for

**Table 1.** Fit results for all hadrons, strange hadrons and non-strange hadrons in central A+A collisions at RHIC and SPS.

| | Pb+Pb at 158 A GeV | | | Au+Au at 200 GeV | | |
|---|---|---|---|---|---|---|
| | All | Strange | Non-strange | All | Strange | Non-strange |
| $\langle\beta\rangle$ (c) | 0.426±0.004 | 0.420±0.007 | 0.442±0.005 | 0.472±0.009 | 0.464±0.006 | 0.463±0.012 |
| $T$ (GeV) | 0.113±0.001 | 0.119±0.004 | 0.109±0.001 | 0.122±0.003 | 0.150±0.005 | 0.107±0.004 |
| $q-1$ | 0.015±0.001 | 0.009±0.004 | 0.015±0.001 | 0.017±0.006 | 0.000±0.002 | 0.039±0.006 |
| $\chi^2$/nDoF | 267/159 | 137/70 | 102/86 | 140/155 | 51/99 | 43/53 |

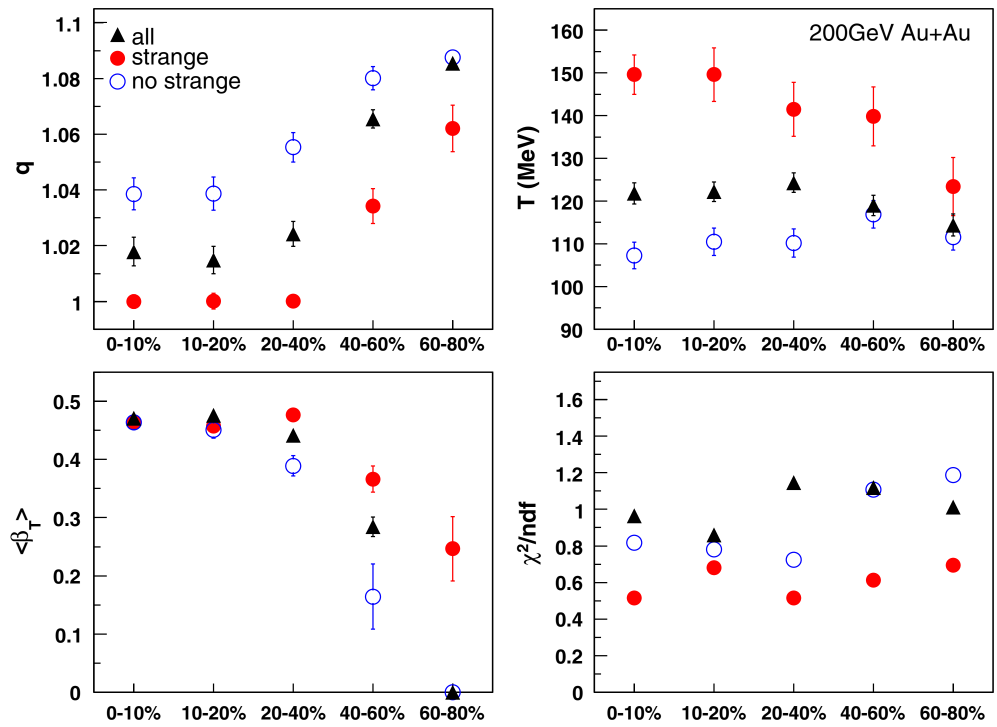


**Figure 4.** $q$, $T$, $\beta$ and $\chi^2$/nDoF as a function of centrality for different groups of hadrons from the TBW model fit to spectra in Au+Au collisions at RHIC top energy.

central nucleus–nucleus collisions at SPS and RHIC. Overall, reasonable $\chi^2$/nDoF is present in all cases. We note that the fits to the strange hadrons produce small $\chi^2$/nDoF ($\sim$0.5), indicating an experimental overestimate of the systematic uncertainty. The strange hadrons consistently show smaller non-equilibrium effect as manifested in a smaller $(q-1)$ value with higher temperature and similar radial flow than the non-strange hadrons. On the other hand, the TBW fit to the strange hadrons at SPS shows larger value of $\chi^2$/nDOF, indicating less than ideal description of the data. In addition, the $\Omega$ and $\bar{\Omega}$ data points have larger fluctuations around the smooth TBW lines than the error bars allow. Figure 4 presents the $q$, $T$ and $\beta$ dependence on the centrality in Au+Au collisions at RHIC top energy. In fact, $(q-1)$ is consistent with zero for strange hadron group and is significantly smaller than that of non-strange hadrons in the 0–40% central Au+Au collisions at RHIC while they approach each other in peripheral bins (40–80%). This is consistent with the findings of [26, 43]: the strangeness saturation factor $\gamma_s$ increases from peripheral to central A+A collisions toward unity at RHIC and SPS top energies, indicating strangeness equilibration in central A+A collisions at RHIC and SPS.

## 3. Discussions

It is clear that the TBW model can provide satisfactory description of the spectra in nucleus–nucleus collisions at RHIC and SPS energies. There are several important conclusions from the results.

(i) The radial flow velocity at SPS is smaller than that at RHIC.
(ii) Freeze-out temperatures for non-strange hadrons are similar at RHIC and SPS.
(iii) The non-equilibrium parameter $(q-1)$ is small in central nucleus–nucleus collisions at RHIC and SPS except a larger $(q-1)$ value for non-strange hadrons at RHIC energy.
(iv) The categorized groups of strange and non-strange hadrons show different parameters, indicating a possible early freeze-out of strange hadrons at RHIC. The biggest difference for strange hadrons from the light hadrons is the freeze-out temperature: strange hadrons freeze out at higher temperature with similar radial flow. A possible conclusion is that the hadronic phase does not increase the radial flow of light hadrons at RHIC energy. The picture at SPS is unclear. Although the strange hadrons have slightly higher temperature, smaller radial flow, and smaller $(q-1)$ than those of the non-strange hadrons, the difference is at about $2\sigma$ level. In addition, the $p_T$ reach for the strange hadrons is considerably lower than those for the non-strange hadrons and the fit quality is less than ideal.
(v) The centrality dependence of $(q-1)$ of strange hadrons shows that the strange hadrons are off-equilibrium in peripheral collisions as other hadrons. However, they approach thermal equilibrium very quickly at middle centrality with very a small $(q-1)$ value.
(vi) Most importantly, the $J/\psi$ spectra at SPS and RHIC require much smaller flow velocity, and much larger off-equilibrium and/or higher temperature than the other hadrons. It also shows that the spectral shapes are the same in $p$+$p$ and central nucleus–nucleus collisions. This is inconsistent with thermal production of $J/\psi$ through recombination of thermal open charms at the chemical freeze-out in the central Au+Au collisions at RHIC [44–47]. On the other hand, a dynamic coalescence throughout the system evolution [48] concludes that $J/\psi$ acquires little flow in the process. This model does not maintain $J/\psi$ in equilibrium and is consistent with our conclusion.

We noted that [18] performed a combined fit to the strange hadrons and $J/\psi$, and concluded that both multi-strange hadrons and $J/\psi$ freeze out early. However, our separate fits provide a different picture, where multi-strange hadrons show deviations from the bulk hadrons with high value of temperature while $J/\psi$ spectral shape shows a little bulk effect, and they are incompatible with each other. The forced combination of these two groups does not provide a good fit, but does produce a set of parameters in-between the separate fit results. We advocate a separate description of strange hadrons and charmed hadrons. Improved data quality with a large kinematic range (especially $\Omega$ spectra at low $p_{\mathrm{T}}$) will provide better fit results for the multi-strange hadrons. A combination of spectra of $J/\psi$ and open charmed hadrons and/or their elliptic flow will enable us to break the correlation among $\beta$, $T$ and $q$. All these improvements await low-energy scan at RHIC, and future charm measurements at FAIR, RHIC and LHC [49–52].

This study also helps clarify the discrepancy on the claims about the early freeze-out of multi-strange hadron using a hydrodynamic evolution and a blast-wave model [5, 7]. In the Boltzmann–Gibbs blast-wave model (BGBW), the obtained $\beta$ for bulk hadrons ($\pi$, K and p) is about 0.6$c$, much larger than what we obtained from the TBW model ($\beta \sim 0.5c$). This may be due to the intrinsic assumption of BGBW where the local thermalization with a Boltzmann distribution increases the radial flow to absorb the non-equilibrium effect. The large $\beta$ apparently increases the difference to that of multi-strange hadrons. On the other hand, it is not clear if freeze-out temperature is the only variable in the final hydrodynamic evolution, where the comparison of $\Omega$ spectrum to the hydrodynamics was made [7]. Usually, it is argued that a hybrid model with hadron cascade at the hadronic phase can describe the experimental data better [53]. A least-$\chi^2$ fit to the spectra using different freeze-out temperature settings in the hydrodynamic model will be valuable at achieving a quantitative comparison among different approaches. Our fit results in figure 4 show that strange hadrons freeze out early but their radial flow is the same as that of light hadrons. This offers an alternative and novel picture of hadron freeze-out.

(i) At the partonic phase, partons approach thermal equilibrium, resulting in a small $(q-1)$ value for strange and light hadrons. However, $J/\psi$ are not thermalized.

(ii) After hadronization, multi-strange hadrons decouple from the system and their measured radial flow reflects that at this stage.

(iii) At the hadronic phase, hadron scattering does not produce a collective radial flow. It is also not sufficient to maintain the system in equilibrium. The consequence is that the copiously produced light hadrons are much further away from the thermal equilibrium at the end of the hadronic phase than at its beginning. This results in a large $(q-1)$ value for light hadrons without increasing the radial flow. this may be a consequence of the explosive nature of the fireball at early stage.

(iv) This type of investigation is not possible with the BGBW since equilibrium is built in its assumption. However, TBW enables us to investigate the effect of non-equilibrium process.

Recently, Tsallis statistics has been applied to extract chemical freeze-out information at RHIC and SPS [6, 54]. However, it shows that the resonance feed-down has a big impact on the minimum $\chi^2$ of the fit [6]. The chemical fit with Tsallis statistics does not produce a meaningful temperature parameter at the minimum $\chi^2$ value when the resonance feed-down is applied. It is tempting to conclude that resonance decays also have a big impact on the spectral shapes of stable hadrons at the kinetic freeze-out [7]. We argue that this is not the case. Models [55, 56], which allow the stable particles to continue the elastic interactions dominantly through resonances after chemical freeze-out, can explain the resonance measurements [19, 20, 57] and the extracted different temperatures between chemical and blast-wave fits [1, 5, 6, 10, 33]. Although the grand total of each stable particle species including those from resonance decay at later time is defined to be a conserved number after chemical freeze-out, for very short-lived resonances produced at chemical freeze-out, most (if not all) of them decay before the kinetic freeze-out. Meanwhile, their daughters from the decays interact with the other bulk hadrons in the medium and the correlation among the daughters as resonance from the chemical freeze-out has been erased. On the other hand, the stable particles and resonances after chemical freeze-out continue the elastic scattering and generate new resonances at a lower rate before kinetic freeze-out. The resonances available at the kinetic freeze-out are those regenerated from the bulk hadrons at the time close to the kinetic freeze-out. Therefore, the resonance yields and kinematics are completely determined by the kinematics of the daughter hadrons that generate those resonances, and not the other way around. As shown in [33], the effect of resonance decay has little impact on the final result. If any, it seems to support the idea that the resonances (i.e. $\rho$) are from regeneration with their yields and kinematics determined by the daughter kinematics.

## 4. Conclusions

Tsallis statistics in a blast-wave model (TBW) was used to investigate the non-Boltzmann distribution, radial flow and freeze-out temperature of particles and their dependence on particle species and beam energy in the relativistic heavy-ion collisions at SPS and RHIC. In addition to the light hadrons, $J/\psi$ and the particles containing strangeness were examined separately to study their radial flow and freeze-out. The $J/\psi$ in Pb+Pb collisions at SPS requires a temperature of 180 MeV and an average flow velocity of 0.06 $c$ in the TBW fit, and therefore is consistent with early decoupling and obtains little radial flow. The $J/\psi$ spectra at RHIC are also inconsistent with the bulk flow profile. However, there is a strong correlation among the obtained parameters from the TBW fit to the $J/\psi$ spectrum alone. To improve the uncertainty and break the parameter correlations, higher statistics, elliptic flow and/or spectra of other charmed hadrons are needed to further determine the detailed $J/\psi$ flow pattern at RHIC. We found that the strange hadrons approach equilibrium quickly from peripheral to central A+A collisions. The temperature from the TBW fit to strange hadrons is higher than that for light hadrons while their radial flows are similar. These results provide a novel picture of freeze-outs: a thermalized system is produced at the partonic phase; the hadronic scattering at later stage is not enough to maintain the system in equilibrium and does not increase the radial flow of the copiously produced light hadrons. The existence of such a picture in reality seems to be natural. However, the investigation of such an off-equilibrium effect has not been possible with the BGBW model or ideal hydrodynamics.

## Acknowledgments

The authors thank Drs Lijuan Ruan, Paul Sorensen, Fuqiang Wang, Pengfei Zhuang, Huanzhong Huang, Gene van Buren, Bedanga Mohanty, Nu Xu, Jean Cleymans and Jun Takahashi for valuable discussions and Dr Enrico Scomparin for providing us with the NA60 $J/\psi$ data points. This work was supported in part by the National Natural Science Foundation of China under grants 10775131, 10805046 and 10835005. Zebo Tang is supported in part by the China Postdoctoral Science Foundation funded project. Zhangbu Xu is supported in part by the PECASE grant and by the grant DE-AC02-98CH10886 from the Offices of NP and HEP within the US DOE Office of Science.

## References

[1] Adams J *et al* 2005 Experimental and theoretical challenges in the search for the quark–gluon plasma: the STAR collaboration's critical assessment of the evidence from RHIC collisions *Nucl. Phys.* A **757** 102–83
[2] Adcox K *et al* 2005 Formation of dense partonic matter in relativistic nucleus–nucleus collisions at RHIC: experimental evaluation by the PHENIX Collaboration *Nucl. Phys.* A **757** 184–283
[3] Arsene I *et al* 2005 Quark gluon plasma an color glass condensate at RHIC? The perspective from the BRAHMS experiment *Nucl. Phys.* A **757** 1–27
[4] Back B B *et al* 2005 The PHOBOS perspective on discoveries at RHIC *Nucl. Phys.* A **757** 28–101
[5] van Hecke H, Sorge H and Xu N 1998 Evidence of early multi-strange hadron freeze-out in high energy nuclear collisions *Phys. Rev. Lett.* **81** 5764–7
[6] Cleymans J 2010 Is strangeness chemically equilibrated? *Int. Conf. on Strangeness in Quark Matter (SQM 2009), J. Phys. G: Nucl. Part. Phys.* at press (arXiv:1001.3002)
[7] Kolb P F and Heinz U W 2003 Hydrodynamic description of ultrarelativistic heavy-ion collisions arXiv:nucl-th/0305084

[8] Tsallis C 1988 Possible generalization of Boltzmann–Gibbs statistics *J. Stat. Phys.* **52** 479–87
[9] Biro T S, Purcsel G and Urmossy K 2009 Non-extensive approach to quark matter *Eur. Phys. J.* A **40** 325–40
[10] Tang Z *et al* 2009 Spectra and radial flow at RHIC with Tsallis statistics in a blast-wave description *Phys. Rev.* C **79** 051901
[11] Wilk G and Wlodarczyk Z 2000 On the interpretation of nonextensive parameter q in Tsallis statistics and Levy distributions *Phys. Rev. Lett.* **84** 2770 (arXiv:hep-ph/9908459)
[12] Wilk G and Wlodarczyk Z 2009 Power laws in elementary and heavy-ion collisions: a story of fluctuations and nonextensivity? *Eur. Phys. J.* A **40** 299–312 (arXiv:0810.2939)
[13] Wilk G and Wlodarczyk Z 2009 Multiplicity fluctuations due to the temperature fluctuations in high-energy nuclear collisions *Phys. Rev.* C **79** 054903 (arXiv:0902.3922)
[14] De B, Bhattacharyya S, Sau G and Biswas S K 2007 Non-extensive thermodynamics, heavy ion collisions and particle production at RHIC energies *Int. J. Mod. Phys.* E **16** 1687–700
[15] Alberico W M, Lavagno A and Quarati P 2000 Non-extensive statistics, fluctuations and correlations in high energy nuclear collisions *Eur. Phys. J.* C **12** 499–506 (arXiv:nucl-th/9902070)
[16] Osada T and Wilk G 2008 Nonextensive hydrodynamics for relativistic heavy-ion collisions *Phys. Rev.* C **77** 044903 (arXiv:0710.1905)
[17] Biro T and Muller B 2004 Almost exponential transverse spectra from power law spectra *Phys. Lett.* B **578** 78–84 (arXiv:hep-ph/0309052)
[18] Petrovici M and Pop A 2009 Collective phenomena in heavy ion collisions arXiv:0904.3666
[19] Adler C *et al* 2002 $K^*(892)^0$ production in relativistic heavy ion collisions at $\sqrt{s_{NN}} = 130$ GeV *Phys. Rev.* C **66** 061901
[20] Adams J *et al* 2005 K*(892) resonance production in Au+Au and *p*+*p* collisions at $\sqrt{s_{NN}} = 200$ GeV at STAR *Phys. Rev.* C **71** 064902
[21] Abelev B I *et al* 2007 Strange particle production in *p*+*p* collisions at $\sqrt{s_{NN}} = 200$ GeV *Phys. Rev.* C **75** 064901
[22] Abelev B I *et al* 2006 Identified baryon and meson distributions at large transverse momenta from Au+Au collisions at $\sqrt{s_{NN}} = 200$ GeV *Phys. Rev. Lett.* **97** 152301
[23] Abelev B I *et al* 2007 Energy dependence of $\pi^{\pm}$, $p$ and $\bar{p}$ transverse momentum spectra for Au+Au collisions at $\sqrt{s_{NN}} = 62.4$ and 200 GeV *Phys. Lett.* B **655** 104–13
[24] Adams J *et al* 2005 Pion, kaon, proton and anti-proton transverse momentum distributions from *p*+*p* and *d*+Au collisions at $\sqrt{s_{NN}} = 200$ GeV *Phys. Lett.* B **616** 8–16
[25] Adams J *et al* 2005 $\phi$ meson production in Au+Au and *p*+*p* collisions at $\sqrt{s_{NN}} = 200$ GeV *Phys. Lett.* B **612** 181–9
[26] Adams J *et al* 2007 Scaling properties of hyperon production in Au+Au collisions at $\sqrt{s_{NN}} = 200$ GeV *Phys. Rev. Lett.* **98** 062301
[27] Adams J *et al* 2006 Identified hadron spectra at large transverse momentum in *p*+*p* and *d*+Au collisions at $\sqrt{s_{NN}} = 200$ GeV *Phys. Lett.* B **637** 161–9
[28] Adler S S *et al* 2004 Identified charged particle spectra and yields in Au+Au collisions at $\sqrt{s_{NN}} = 200$ GeV *Phys. Rev.* C **69** 034909
[29] Adare A *et al* 2007 $J/\psi$ production versus transverse momentum and rapidity in *p*+*p* collisions at $\sqrt{s} = 200$ GeV *Phys. Rev. Lett.* **98** 232002
[30] Adare A *et al* 2008 $J/\psi$ Production in sqrt $\sqrt{s_{NN}} = 200$ GeV Cu+Cu Collisions *Phys. Rev. Lett.* **101** 122301
[31] Adare A *et al* 2007 $J/\psi$ production vs centrality, transverse momentum, and rapidity in Au+Au collisions at $\sqrt{s_{NN}} = 200$ GeV *Phys. Rev. Lett.* **98** 232301
[32] Abelev B I *et al* 2009 $J/\psi$ production at high transverse momentum in *p*+*p* and Cu+Cu collisions at $\sqrt{s_{NN}} = 200$ GeV *Phys. Rev.* C **80** 041902
[33] Abelev B I *et al* 2009 Systematic measurements of identified particle spectra in *p*+*p*, *d*+Au and Au+Au collisions from STAR *Phys. Rev.* C **79** 034909
[34] Alt C *et al* 2008 High transverse momentum hadron spectra at $\sqrt{s_{NN}} = 17.3$ GeV, in Pb+Pb and p+p collisions, measured by CERN-NA49 *Phys. Rev.* C **77** 034906
[35] Alt C *et al* 2008 Energy dependence of $\Lambda$ and $\Xi$ production in central Pb+Pb collisions at A-20, A-30, A-40, A-80, and A-158 GeV measured at the CERN super proton synchrotron *Phys. Rev.* C **78** 034918
[36] Alt C *et al* 2005 $\Omega^-$ and $\bar{\Omega}^+$ production in central Pb+Pb collisions at 40 A GeV and 158 A GeV *Phys. Rev. Lett.* **94** 192301
[37] Anticic T *et al* 2004 Energy and centrality dependence of deuteron and proton production in Pb+Pb collisions at relativistic energies *Phys. Rev.* C **69** 024902
[38] Alt C *et al* 2008 Energy dependence of phi meson production in central Pb+Pb collisions at $\sqrt{s_{NN}} = 6$ to 17 GeV *Phys. Rev.* C **78** 044907

[39] Abreu M C *et al* 2001 Transverse momentum distributions of $J/\psi$, $\psi'$, Drell–Yan and continuum dimuons produced in Pb+Pb interactions at the SPS *Phys. Lett.* B **499** 85–96
[40] Antinori F *et al* 2004 Study of the transverse mass spectra of strange particles in Pb+Pb collisions at 158 AGeV *J. Phys. G: Nucl. Part. Phys.* **30** 823–40
[41] Bruno G E 2005 Blast-wave analysis of strange particle $m_T$ spectra in Pb+Pb collisions at the SPS *J. Phys. G: Nucl. Part. Phys.* **31** S127–34
[42] Scomparin E 2007 $J/\psi$ production in In+In and $p$+A collisions *J. Phys. G: Nucl. Part. Phys.* **34** S463–70
[43] Becattini F, Gazdzicki M, Keranen A, Manninen J and Stock R 2004 Study of chemical equilibrium in nucleus nucleus collisions at AGS and SPS energies *Phys. Rev.* C **69** 024905
[44] Andronic A, Braun-Munzinger P, Redlich K and Stachel J 2007 Statistical hadronization of heavy quarks in ultra-relativistic nucleus–nucleus collisions *Nucl. Phys.* A **789** 334–56
[45] Ravagli L and Rapp R 2007 Quark coalescence based on a transport equation *Phys. Lett.* B **655** 126–31
[46] Thews R L 2005 Quarkonium formation in statistical and kinetic models *Eur. Phys. J.* C **43** 97–102
[47] Linnyk O, Bratkovskaya E L and Cassing W 2008 Evidence for non-hadronic interactions of charm degrees of freedom in heavy-ion collisions at relativistic energies *Nucl. Phys.* A **807** 79–104
[48] Yan L, Zhuang P and Xu N 2006 Competition between $J/\psi$ suppression and regeneration in quark–gluon plasma *Phys. Rev. Lett.* **97** 232301
[49] Bouchet J 2009 Heavy flavor tracker (HFT): a new inner tracking device at STAR arXiv:0907.3407
[50] van Hecke H 2008 Measuring charm and bottom using the PHENIX silicon vertex detectors *J. Phys. G: Nucl. Part. Phys.* **35** 104146
[51] Dainese A 2007 Charm and beauty at the LHC *Nucl. Phys.* A **783** 417–25
[52] Heuser J M 2009 The compressed baryonic matter experiment at FAIR: progress with feasibility studies and detector developments arXiv:0907.2136
[53] Teaney D, Lauret J and Shuryak E V 2001 A hydrodynamic description of heavy ion collisions at the SPS and RHIC arXiv:nucl-th/0110037
[54] Cleymans J, Hamar G, Levai P and Wheaton S 2008 Near-thermal equilibrium with Tsallis distributions in heavy ion collisions, arXiv:0812.1471
[55] Bleicher M 2003 Probing hadronization and freeze-out with multiple strange hadrons and strange resonances *Nucl. Phys.* A **715** 85–94
[56] Torrieri G and Rafelski J 2001 Strange hadron resonances as a signature of freeze-out dynamics *Phys. Lett.* B **509** 239–45
[57] Adams J *et al* 2006 Strange baryon resonance production in $\sqrt{s_{NN}} = 200$ GeV $p$+$p$ and Au+Au collisions *Phys. Rev. Lett.* **97** 132301